CHEMISTRY
A European Journal

Supporting Information

Sequence-Dependent Duplex Stabilization upon Formation of a Metal-Mediated Base Pair

Philipp Scharf,[a, b] Biswarup Jash,[a, c] Jissy A. Kuriappan,[d] Mark P. Waller,[d] and Jens Müller*[a, c]

chem_201503405_sm_miscellaneous_information.pdf

Synthesis of (*S*)-1-(4,4'-dimethoxytrityl)-3-(1*H*-imidazo[4,5-*f*][1,10]phenanthrolin-1-yl)propan-2-ol (*S*)-3. 1*H*-imidazo[4,5-*f*][1,10]phenanthroline **1** (531.5 mg, 2.413 mmol) and NaH (60% in mineral oil, 23.4 mg, 0.585 mmol) were suspended in dry DMF (5 mL). After stirring for 1 h at room temperature, (*S*)-glycidyl 4,4'-dimethoxytrityl ether (*S*)-**2** (1386 mg, 3.682 mmol) in dry DMF (10 mL) was added. The mixture was stirred for 18 h at 110 °C. After removing the solvent in vacuo, the syrup was treated with ethyl acetate, and the precipitate was filtered off. After removal of the solvent, compound (*S*)-**3** was purified by column chromatography (SiO_2, DCM/MeOH/Et_3N (6/1/0.01)) and was obtained as an off-white foam (1.12 g, 1.88 mmol, 78 %). Elemental analysis: calcd. (%) for $C_{37}H_{32}N_4O_4 \cdot 0.25\ CH_2Cl_2$: C 72.4, H 5.3, N 9.1, found: C 72.5, H 5.5, N 9.0. $[\alpha]_D^{20} = -21.6$ (*c* = 1 in CH_3OH). ^{1}H NMR (400 MHz, CD_2Cl_2): δ = 8.56 – 8.48 (m, 2H, H2, H9), 8.46 – 8.33 (m, 2H, H4, H7), 7.79 (s, 1H, $H2_{imi}$), 7.66 – 7.62 (m, 2H, DMT_{ortho}), 7.55 – 7.51 (m, 4H, DMT_{ortho}), 7.43 (dd, *J* = 8.5 Hz, 6.9 Hz, 2H, DMT_{meta}), 7.36 – 7.30 (m, 2H, H3, DMT_{para}), 7.23 (dd, *J* = 8.3 Hz, 4.2 Hz, 1H, H8), 6.99 – 6.93 (m, 4H, DMT_{meta}), 5.05 – 4.90 (m, 2H, H1', H1''), 4.25 – 4.16 (m, 1H, H2'), 3.83 (s, 6H, 2 × CH_3), 3.80 – 3.72 (m, 1H, H3' or H3''), 3.48 – 3.39 (m, 1H, H3'' or H3') ppm. ^{13}C NMR (101 MHz, CD_2Cl_2): δ = 159.4 (DMT), 148.3 (C2), 146.9 (C9), 145.6 (C1a), 144.9 (DMT), 144.7 (C10a), 143.1 (C2imi), 142.0 (C5), 137.0 (DMT), 136.4 (DMT), 130.8 (DMT), 129.0 (DMT), 128.5 (C4), 127.2 (C7), 123.8 (DMT), 123.2 (DMT), 122.3 (C4a), 119.8 (C3), 119.4 (C6a), 113.5 (C6), 113.5 (C8), 113.4 (DMT), 87.1 (DMT), 67.4 (C2'), 66.5 (C3'), 55.8 (2 × CH_3), 54.0 (C1') ppm. HRMS: m/z $[M+H]^+$ calcd. for $C_{37}H_{33}N_4O_4$: 597.2496, found: 597.2476.

Synthesis of (*S*)-1-(4,4'-dimethoxytrityl)-3-(1*H*-imidazo[4,5-*f*][1,10]phenanthrolin-1-yl)propan-2-yl (2-cyanoethyl) diisopropylphosphoramidite (*S*)-4. To a solution of compound (*S*)-**3** (730 mg, 1.22 mmol) and diisopropyethylamine (1.10 mL, 6.31 mmol) in dry DCM (20 mL) *N*,*N*-diisopropylchlorophosphoramidite (600 µL, 2.69 mmol) was added. After 1 h, the reaction mixture was poured into saturated aqueous $NaHCO_3$ solution and extracted with DCM (2 × 25 mL). The organic layer was dried ($MgSO_4$) and evaporated. The residue was purified by chromatography (SiO_2, DCM/MeOH/Et_3N (12/1/0.1)), affording (*S*)-**4** as a mixture of diastereomers of as a colorless oil (436 mg, 0.55 mmol). ^{1}H NMR (400 MHz, CD_2Cl_2): δ = 9.10 – 9.05 (m, 2H, H2, H9), 8.97 – 8.89 (m, 2H, H4, H7), 7.97 (s, 0.5H, $H2_{imi}$), 7.94 (s, 0.5H, $H2_{imi}$), 7.73 – 7.67 (m, 2H, H3, H8), 7.57 – 7.50 (m, 2H, DMT_{ortho}), 7.48 – 7.27 (m, 7H, DMT_{ortho}, DMT_{meta}, DMT_{para}), 6.92 – 6.82 (m, 4H, DMT_{meta}), 5.24 – 5.05 (m, 1H, H1' or H1''), 4.64 –4.38 (m, 2H, H1'' or H1', H2'), 4.60 – 4.45 (m, 2H, OCH_2), 3.80 (s, 3H, OCH_3), 3.79 (s, 3H, OCH_3), 3.61 – 3.25 (m, 4H, 2 × ^{i}Pr-CH, H3', H3''), 2.34 – 2.12 (m, 2H, CH_2CN), 1.00 – 0.78 (m, 12H, 4 × ^{i}Pr-CH_3) ppm. ^{31}P NMR (81 MHz, CD_2Cl_2): δ = 150.2, 149.8 ppm. HRMS: m/z $[M+H]^+$ calcd. for $C_{46}H_{50}N_6O_5P$: 797.3575, found: 797.3555.

Table S1. Glycosidic torsion angle derived from the QM/MM-optimized structures of duplexes **I** and **II** as shown in Figure 3 (for the central five base pairs).[1] All nucleobases are oriented *anti* with respect to their sugar moiety.

	duplex **I**			duplex **II**		
entry	base pair	angle / ° (base 1)	angle / ° (base 2)	base pair	angle / ° (base 1)	angle / ° (base 2)
1	G:C	255.3	217.3	G:C	208.6	247.1
2	A:T	262.3	216.1	A:T	276.7	215.3
3	**X**–Ag(I)–**P**	226.1	155.0	**P**–Ag(I)–**X**	126.8	246.6
4	A:T	217.0	239.0	A:T	249.9	252.9
5	G:C	240.9	206.0	G:C	234.1	212.8

Table S2. Structural data derived from the QM/MM-optimized structures of duplexes **I** and **II** as shown in Figure 3 (C1'···C1' distance and dihedral angle between complementary nucleobases).

	duplex **I**			duplex **II**		
entry	base pair	C1'···C1' / Å	angle / °	base pair	C1'···C1' / Å	angle / °
1	G:C	10.3	2.4	G:C	10.3	2.4
2	A:T	10.8	10.1	A:T	10.5	11.3
3	G:C	10.6	11.4	G:C	10.9	12.1
4	G:C	10.7	15.0	G:C	10.5	22.0
5	G:C	10.3	24.0	G:C	10.7	20.2
6	A:T	10.7	15.7	A:T	13.3	31.1
7	**X**–Ag(I)–**P**	12.9	16.7	**P**–Ag(I)–**X**	12.8	28.9
8	A:T	11.3	16.3	A:T	11.0	11.5
9	G:C	10.7	18.9	G:C	10.7	13.0
10	A:T	10.7	22.5	A:T	10.7	22.7
11	A:T	10.7	23.7	A:T	10.8	18.5
12	A:T	10.6	20.8	A:T	10.7	13.7
13	G:C	10.1	2.6	G:C	10.1	2.5

Table S3. Hydrogen-bond distances and coordinate bond lengths derived from the QM/MM-optimized structures of duplexes **I** and **II** as shown in Figure 3 (for the central five base pairs).

		Duplex **I**	Duplex **II**
base pair	atoms	distance / Å	distance / Å
G:C	O···HN	2.15	1.92
	NH···N	1.91	1.89
	NH···O	1.81	1.82
	O···N	3.14	2.91
	N···N	2.90	2.87
	N···O	2.77	2.82
A:T	NH···O	1.86	4.68
	NH···N	1.88	4.67
	N···O	2.86	5.68
	N···N	2.89	5.62
X–Ag(I)–**P** or **P**–Ag(I)–**X**	N1–Ag	2.34	2.30
	N10–Ag	2.32	2.34
	N_{imi}–Ag	2.16	2.14
A:T	NH···O	1.85	1.76
	NH···N	2.15	1.99
	N···O	2.82	2.75
	N···N	3.13	2.99
G:C	O···HN	1.99	1.87
	NH···N	1.90	1.92
	NH···O	1.83	1.82
	O···N	2.93	2.87
	N···N	2.89	2.91
	N···O	2.84	2.84

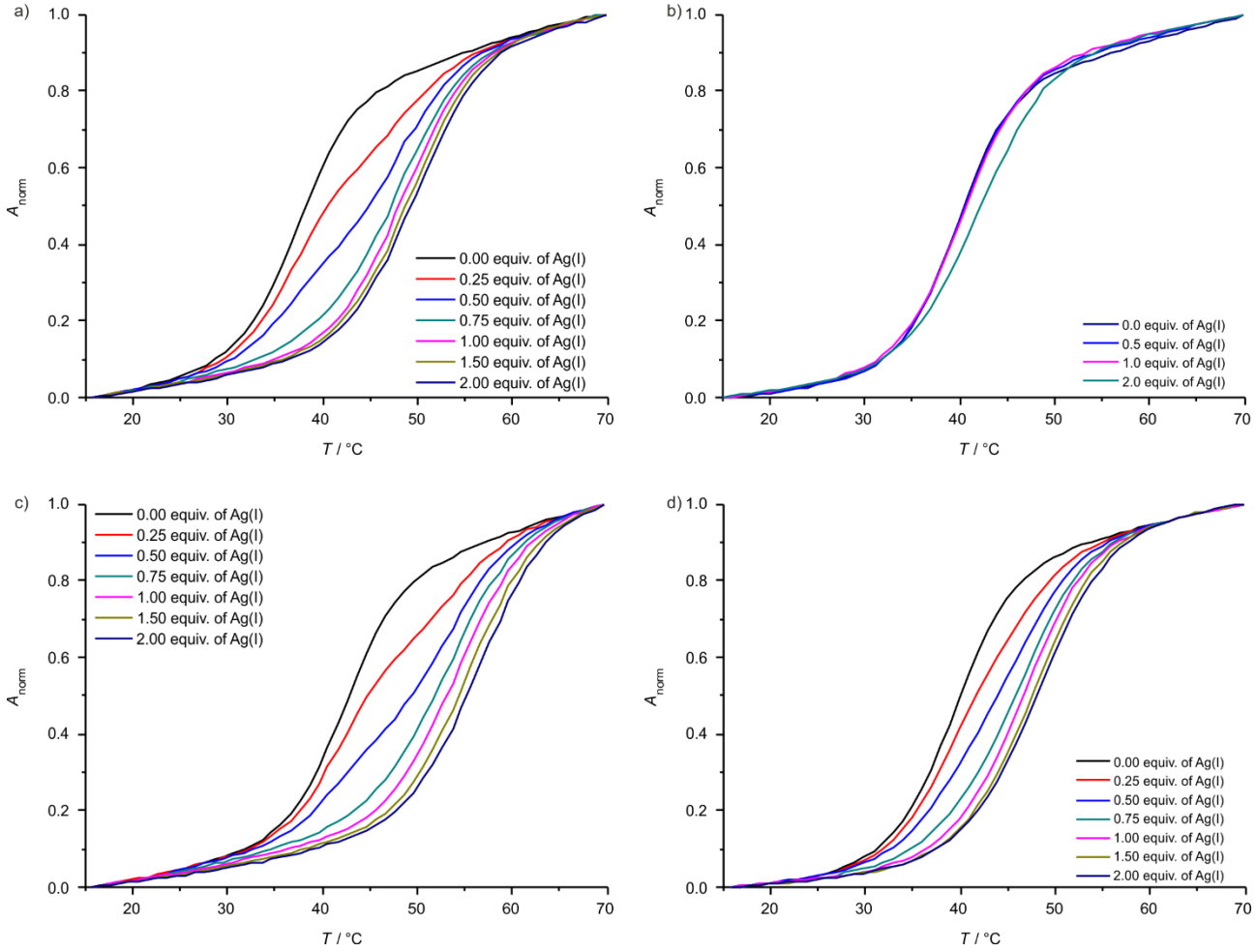

Figure S1. Melting curves of a) duplex **I**, b) duplex **II**, c) duplex **III**, and d) duplex **IV** in the presence of increasing amounts of $AgNO_3$. The absorbance was normalized according to $A_{norm} = (A - A_{min})/(A_{max} - A_{min})$ at 260 nm. Melting temperatures have been determined as the maximum of the derivative of the annealing curves. The biphasic melting behavior in the presence of substoichiometric amounts of $AgNO_3$ can be explained when assuming that the metal-mediated base pair is kinetically inert. Hence, a mixture of metal-free and metal-containing duplexes exists in solution that do not exchange the metal ions within the time scale of the experiment.

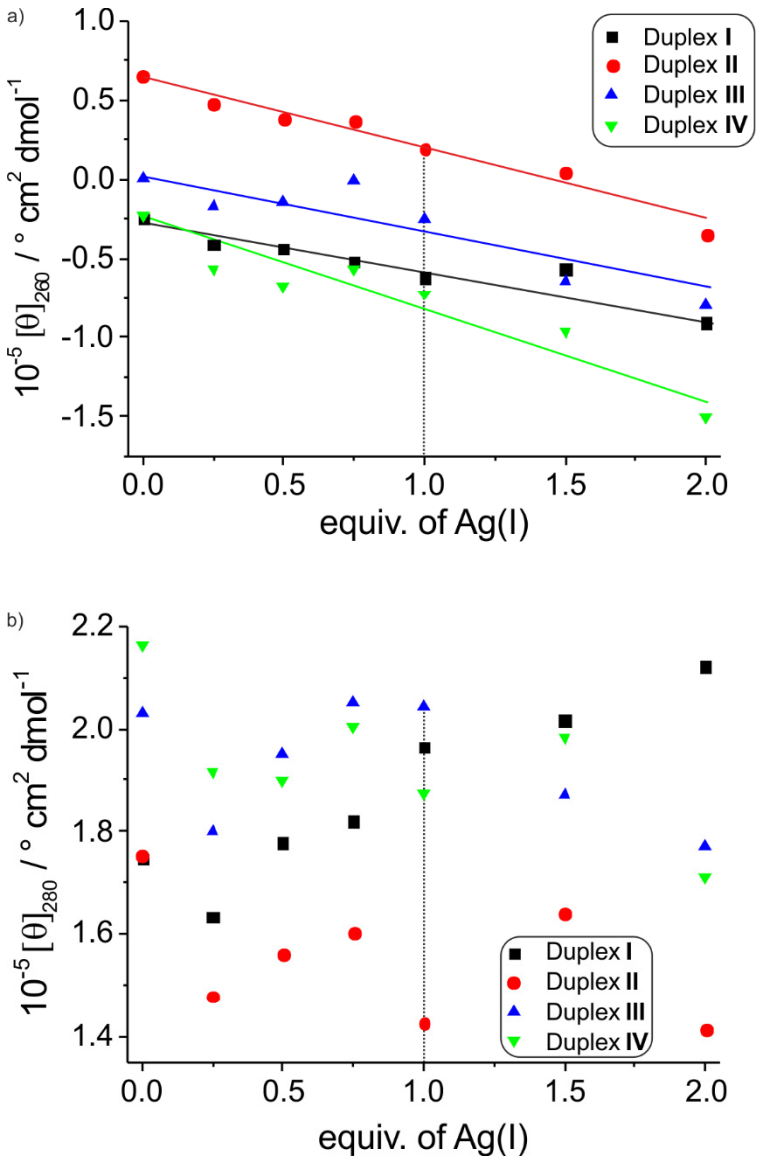

Figure S2. Plot of the molar ellipticity at a) 260 nm and b) 280 nm versus the added amounts of $AgNO_3$. The stoichiometry of metal ion and base pair cannot be determined from these plots.

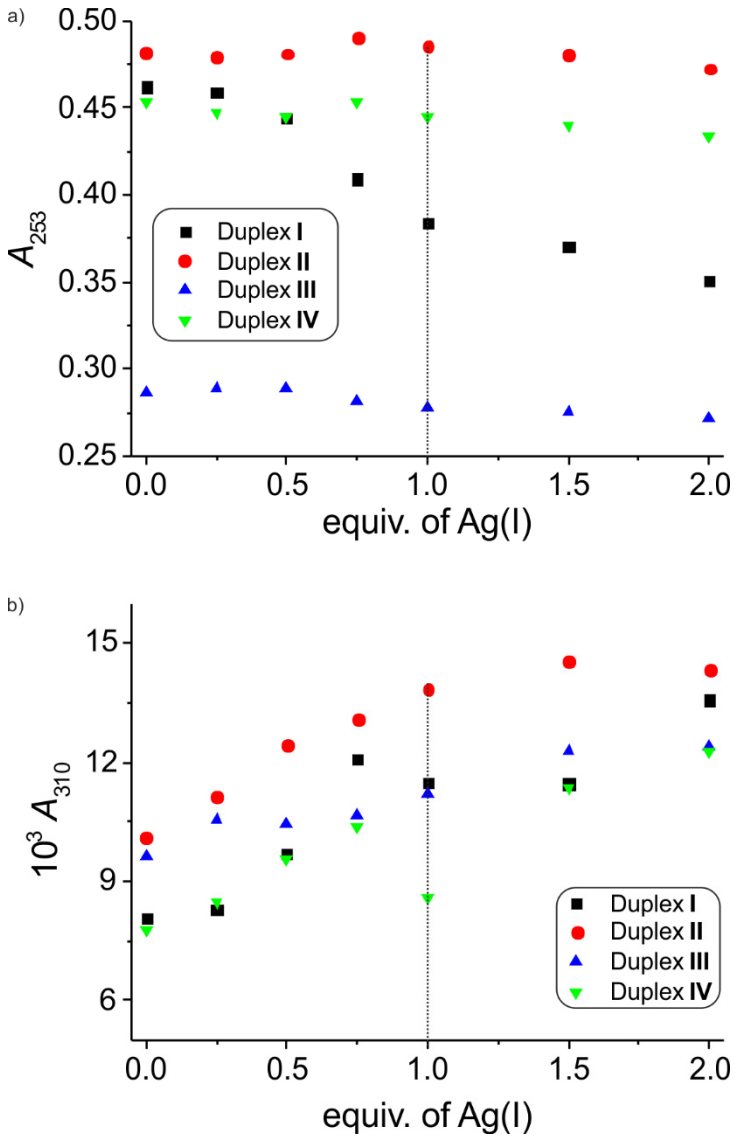

Figure S3. Plot of the absorbance at a) 253 nm and b) 310 nm versus the added amounts of $AgNO_3$. The stoichiometry of metal ion and base pair cannot be determined from these plots.

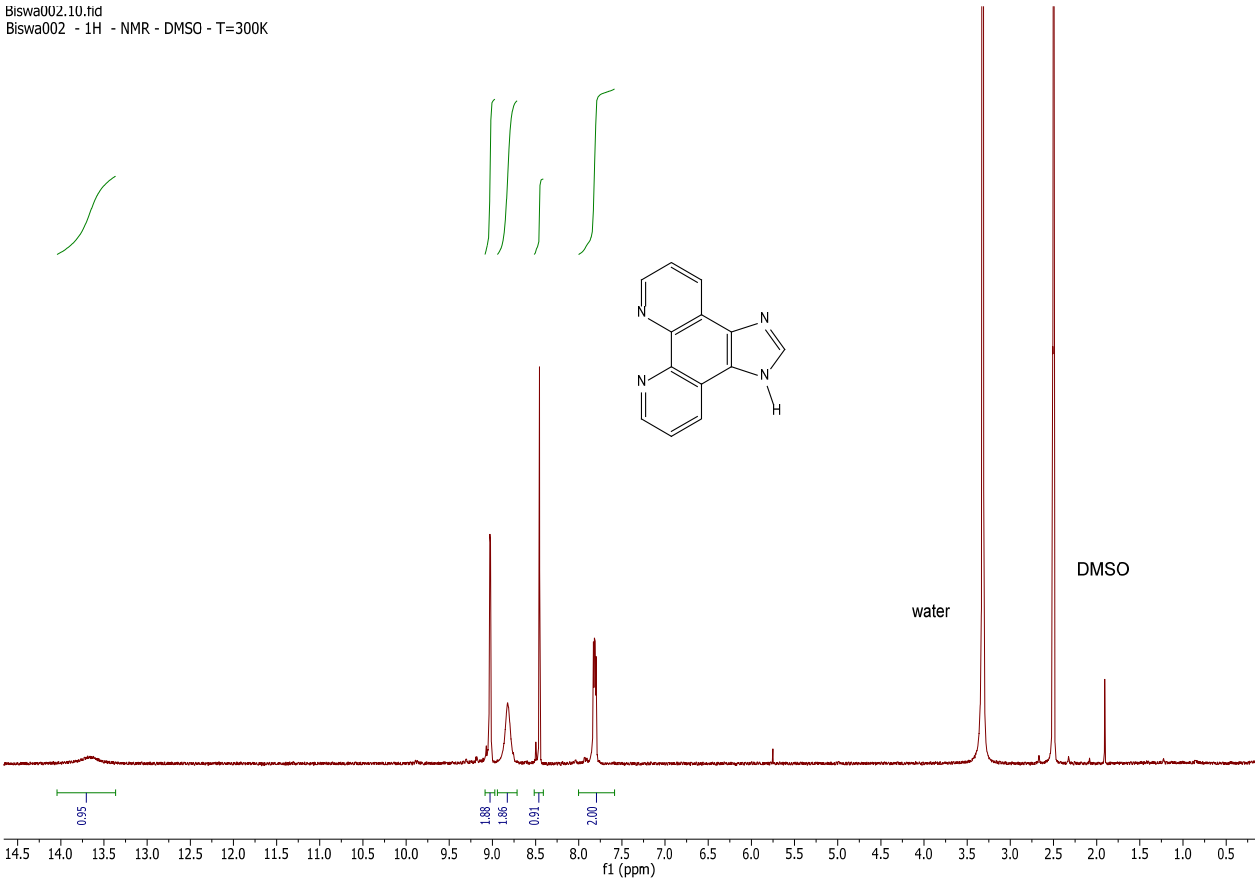

Figure S4. ^{1}H NMR spectrum of compound **1**.

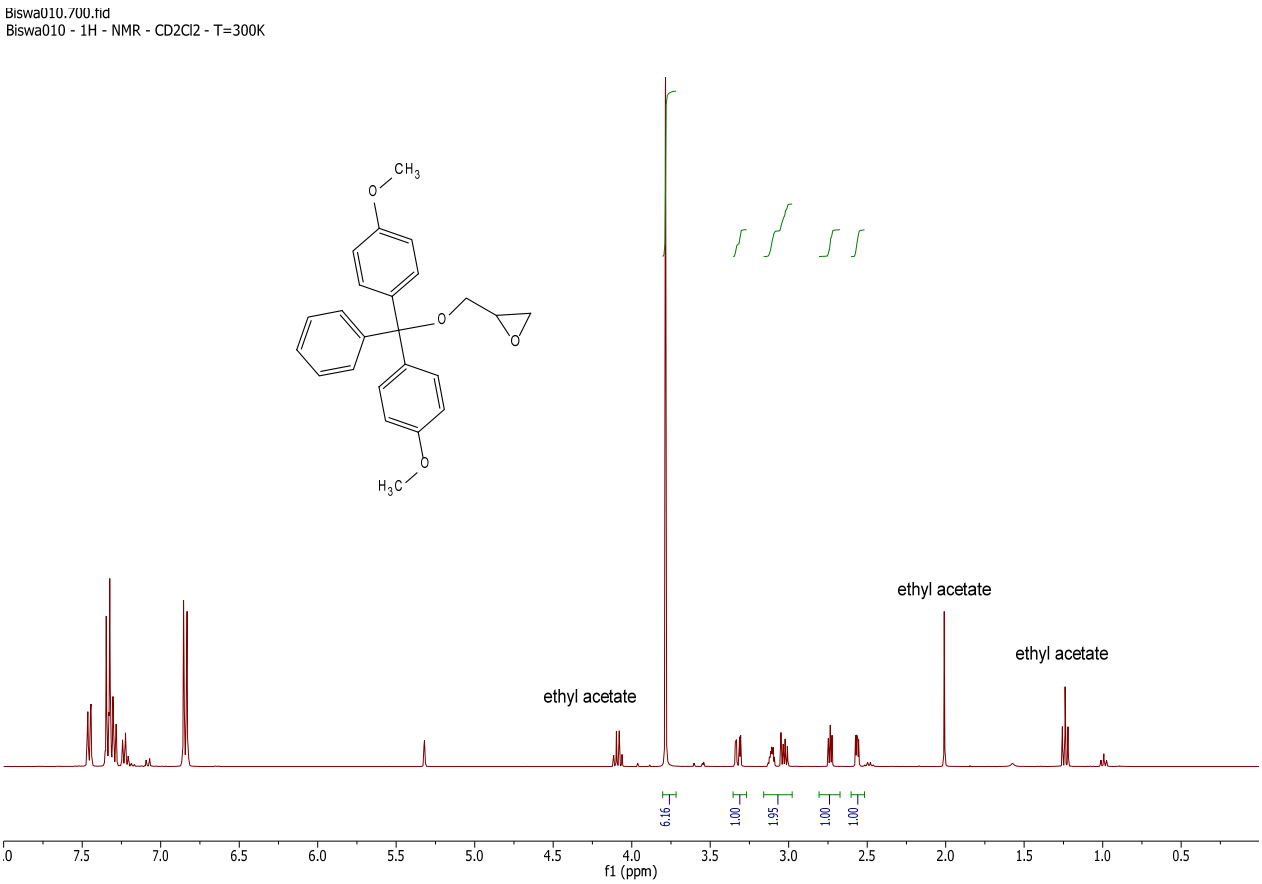

Figure S5. ^{1}H NMR spectrum of compound (*S*)-**2**.

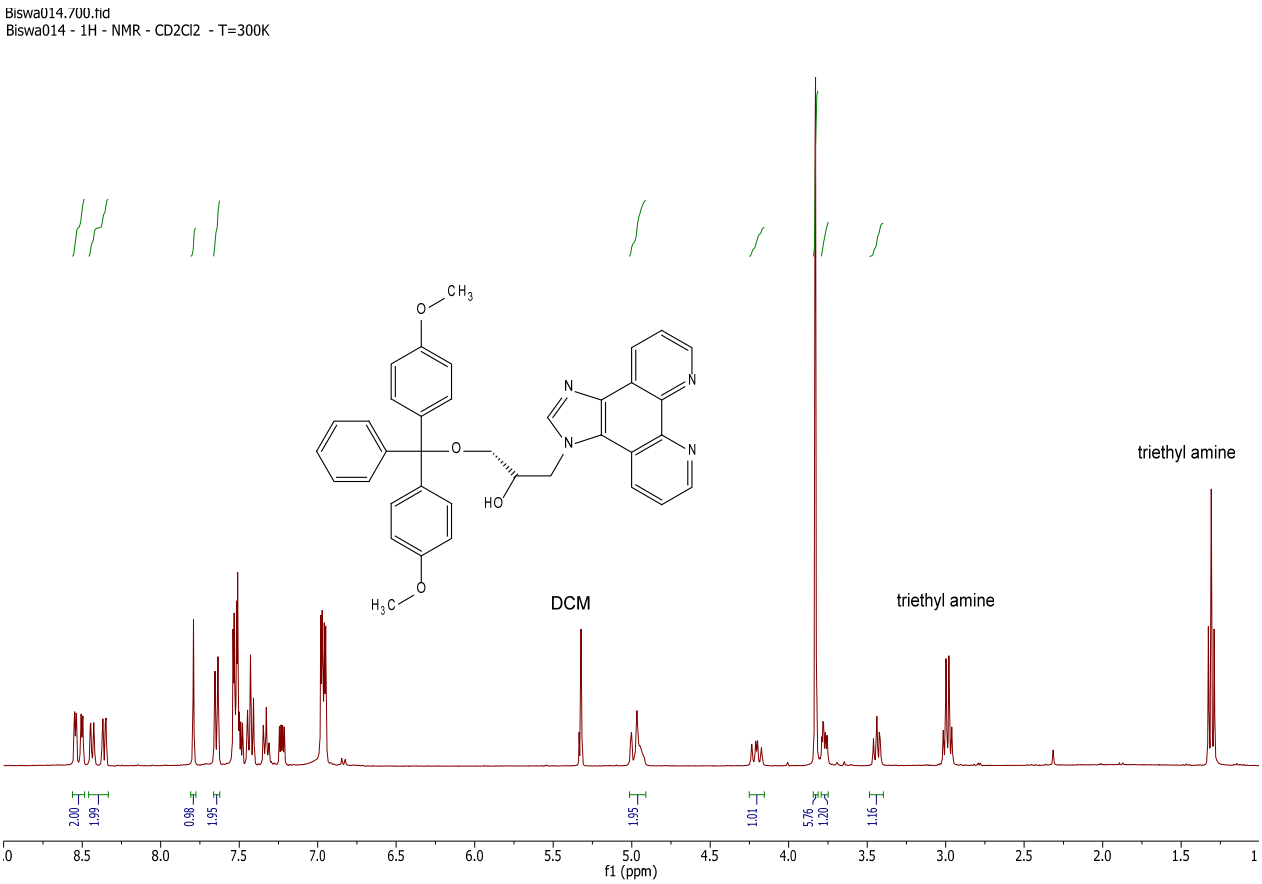

Figure S6. ^{1}H NMR spectrum of compound (*S*)-**3**.

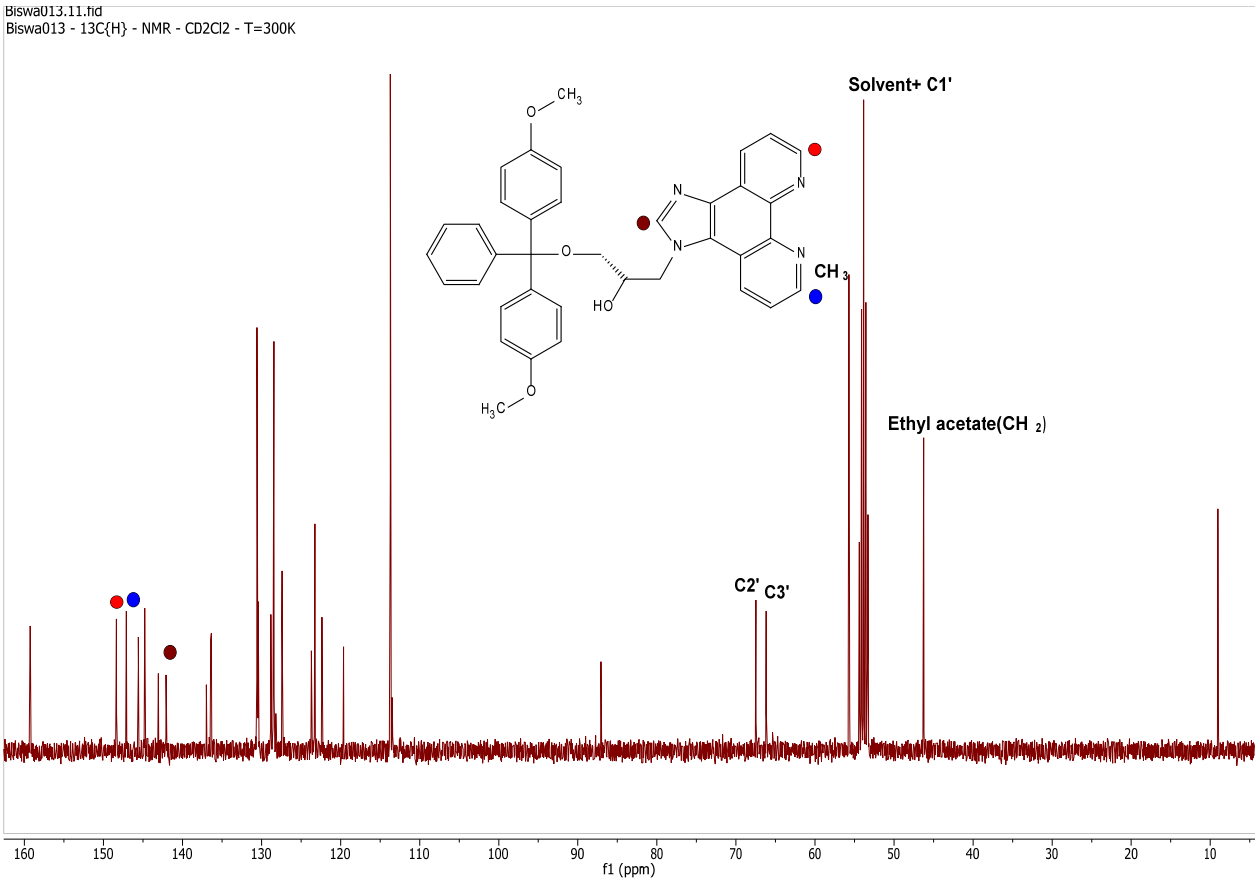

Figure S7. ^{13}C NMR spectrum of compound (*S*)-**3**.

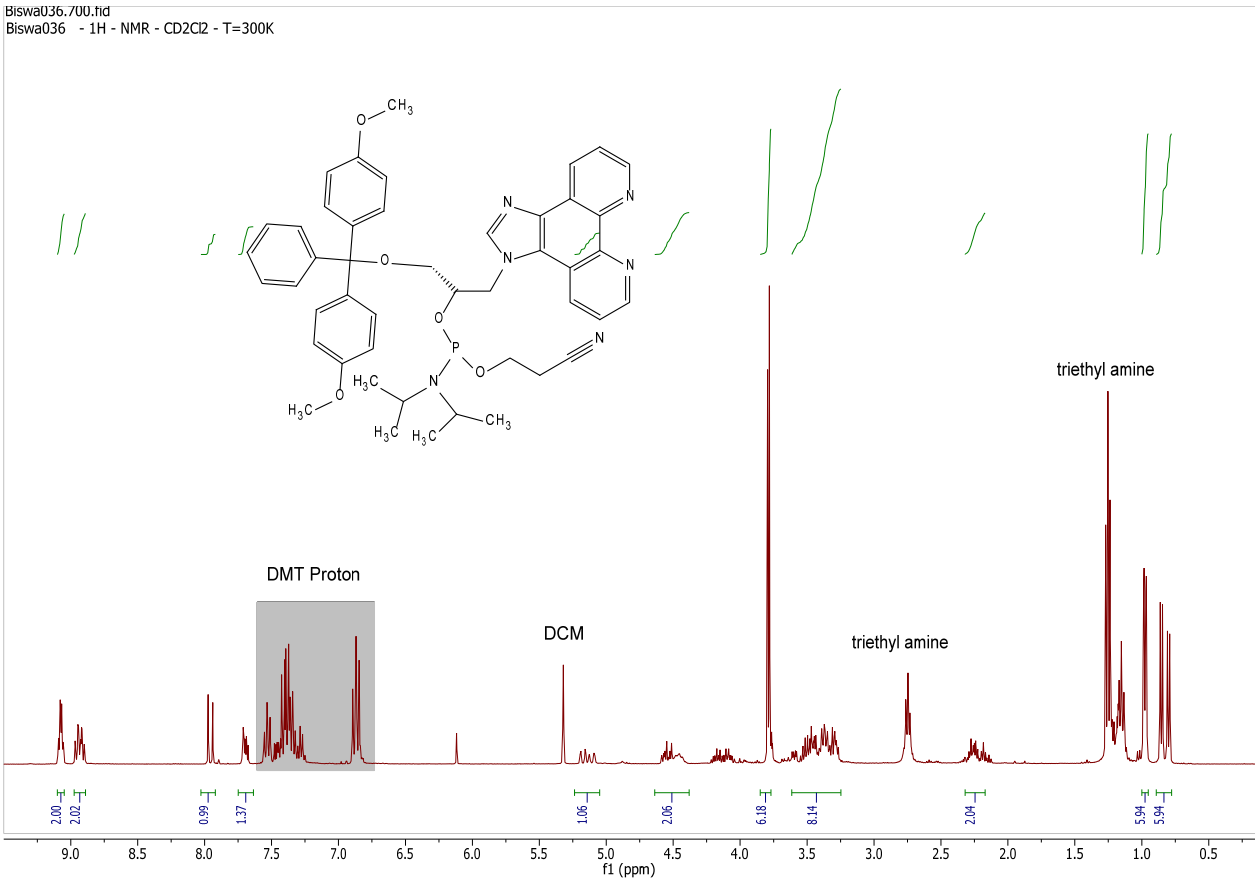

Figure S8. ^{1}H NMR spectrum of compound (*S*)-**4**.

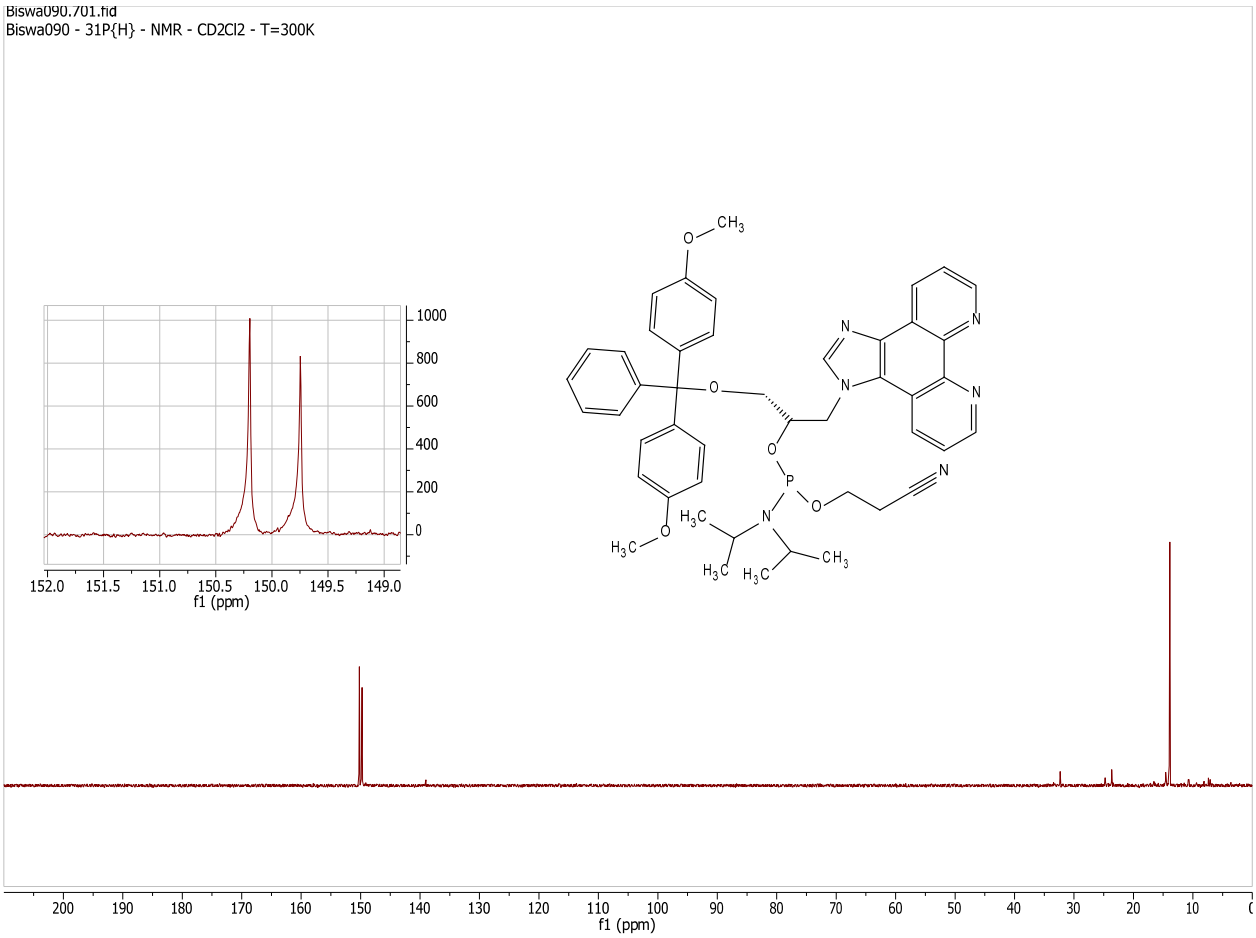

Figure S9. ^{31}P NMR spectrum of compound (*S*)-**4**.

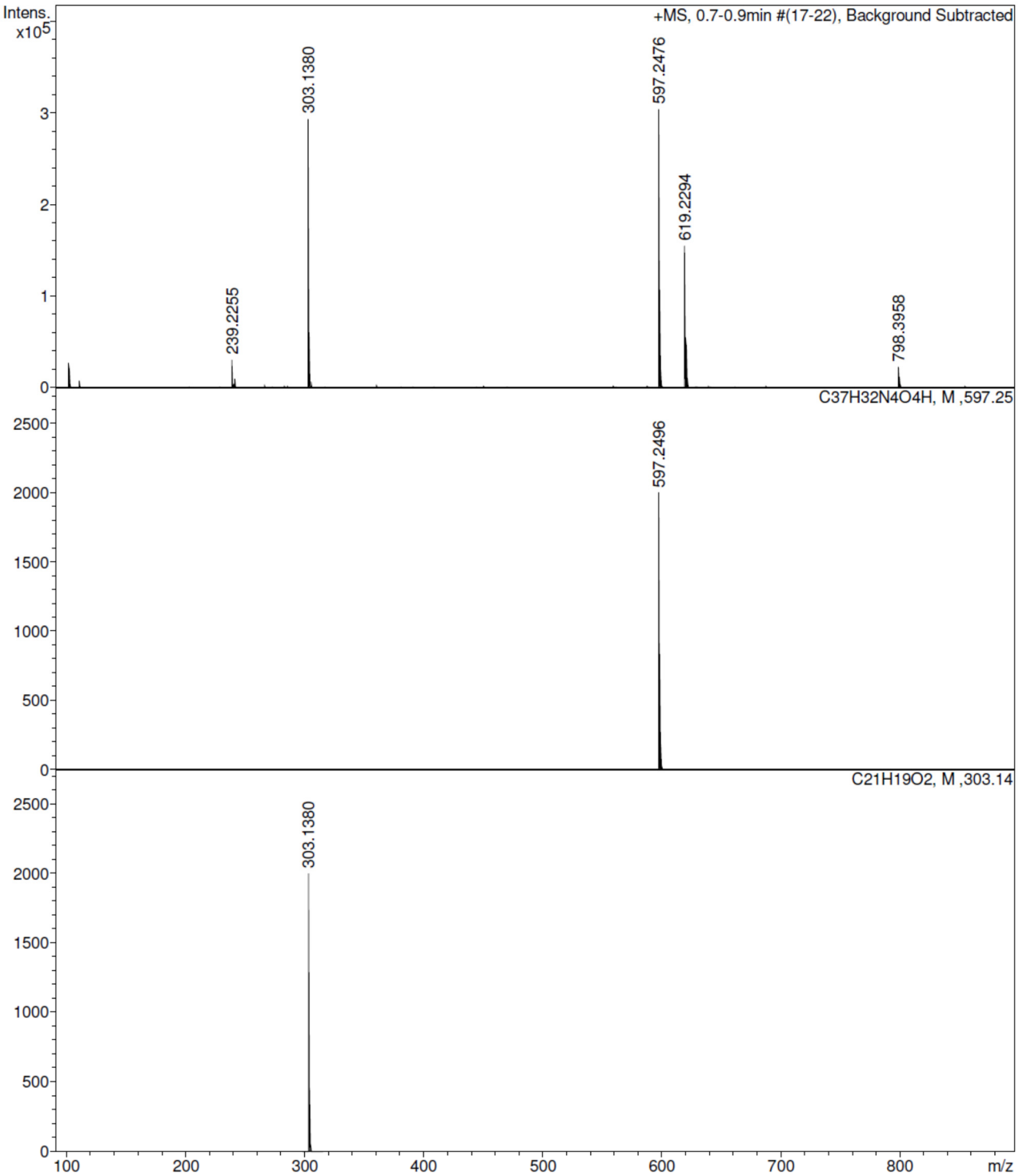

Figure S10. Mass spectrum of compound (*S*)-**3** (top: experimental; middle: computed for [**3**+H]$^+$; bottom: computed for DMT cation).

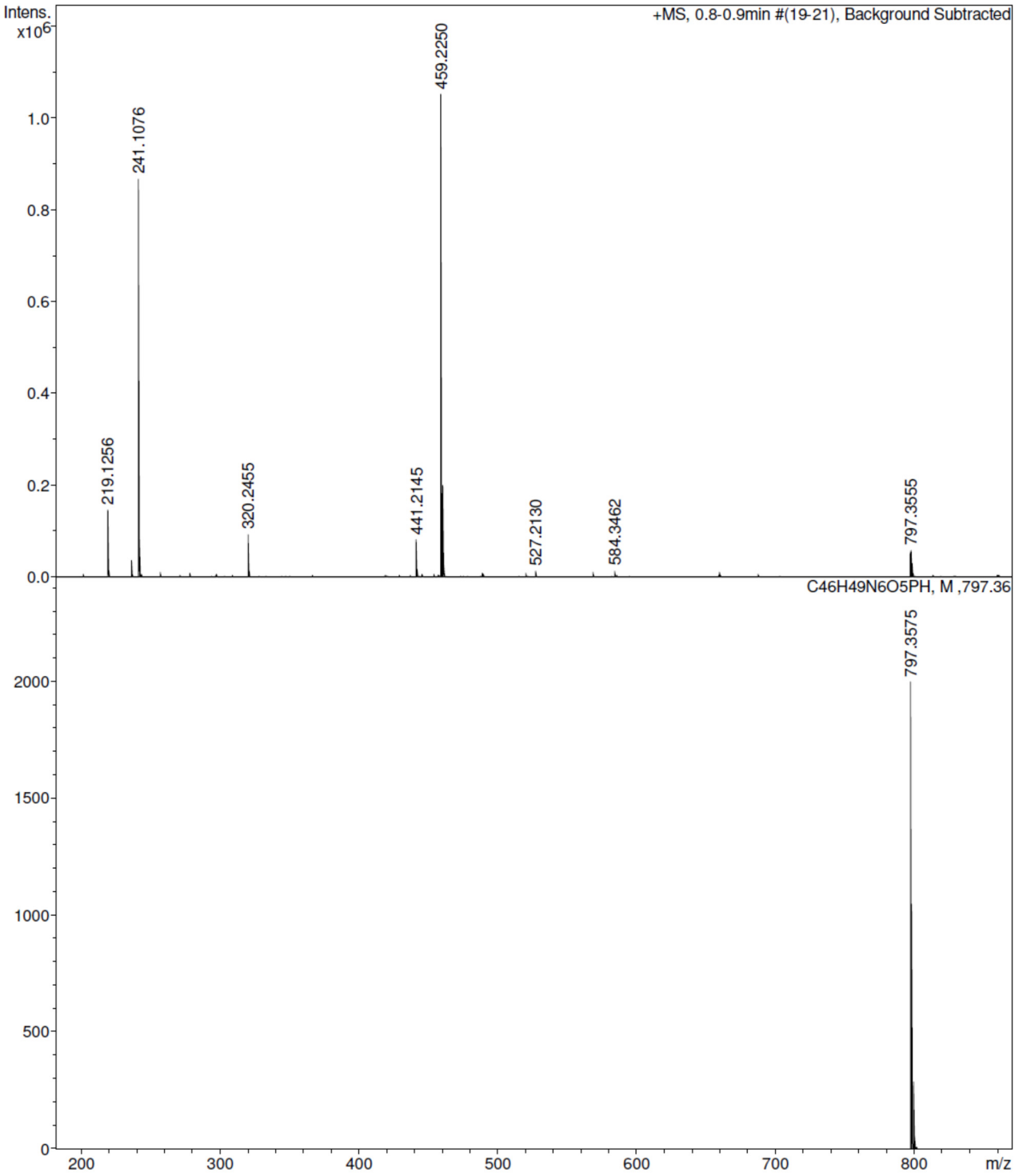

Figure S11. Mass spectrum of compound (*S*)-**4** (top: experimental; bottom: computed for [**4**+H]$^+$).

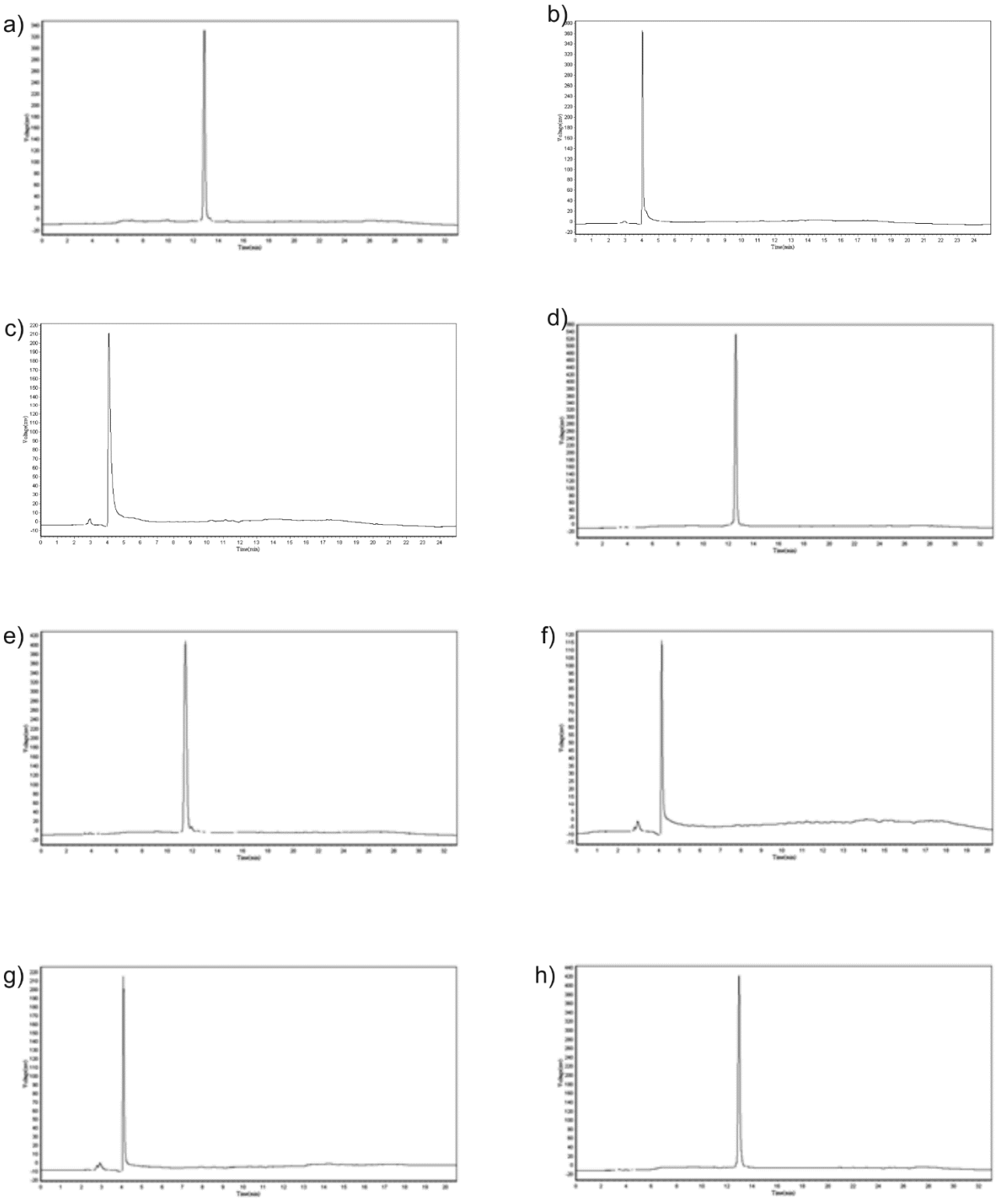

Figure S12. HPLC traces of purified oligonucleotides a) ODN1, b) ODN2, c) ODN3, d) ODN4, e) ODN5, f) ODN6, g) ODN7, h) ODN8; *x* and *y* axes show the retention time and the UV absorbance at 260 nm, respectively. An RP-18 column (250 mm, 10 μm) was used in combination with the following eluents at a flow rate of 0.75 mL mol^{-1}: CH_3CN (solvent A) and 0.1 M aqueous triethylammonium acetate (pH 7.0) : CH_3CN (95:5) (solvent B). Gradient applied for oligonucleotides containing the artificial nucleoside **X**: 0-20 min, 0-20% A; 20-25 min, 20% A; 25-30 min, 20-0% A. Gradient applied for oligonucleotides containing the artificial nucleoside analog **P**: 0-3 min, 10-15% A; 3-15 min, 15-50% A; 15-20 min, 50-10% A.

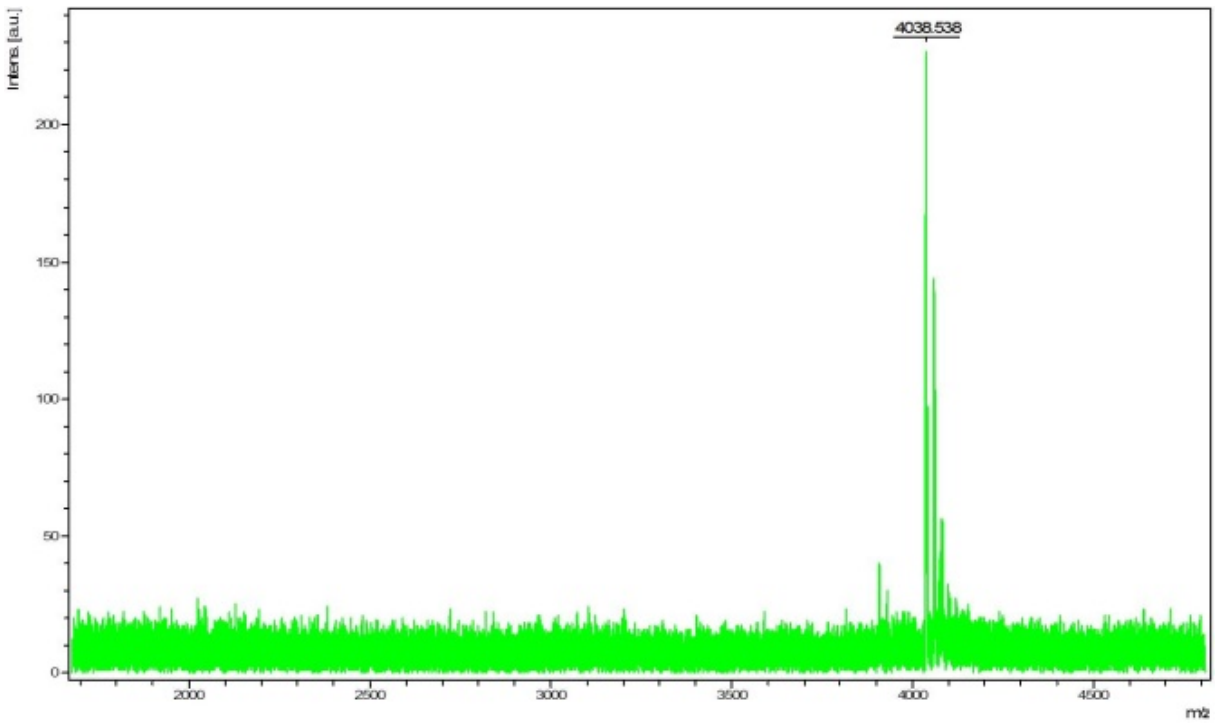

Figure S13. MALDI-ToF spectra of ODN1 (calcd. for $[M+H]^+$: 4038 Da).

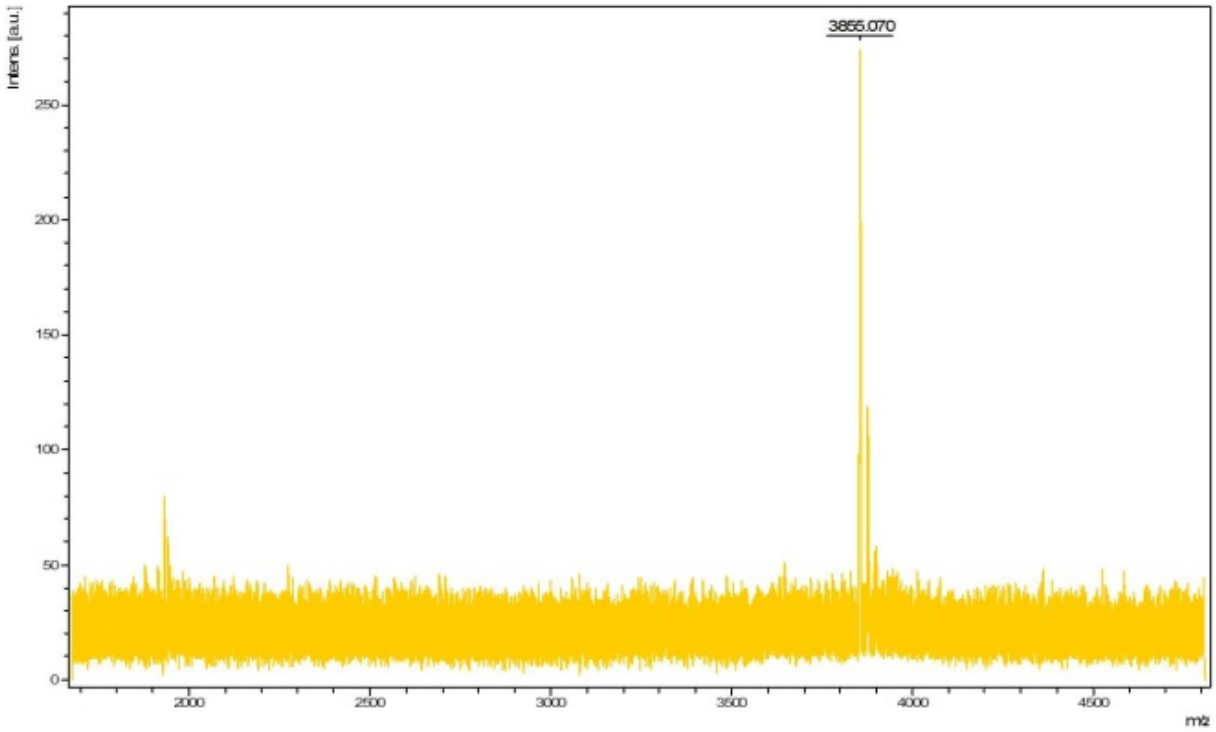

Figure S14. MALDI-ToF spectra of ODN2 (calcd. for $[M+H]^+$: 3854 Da).

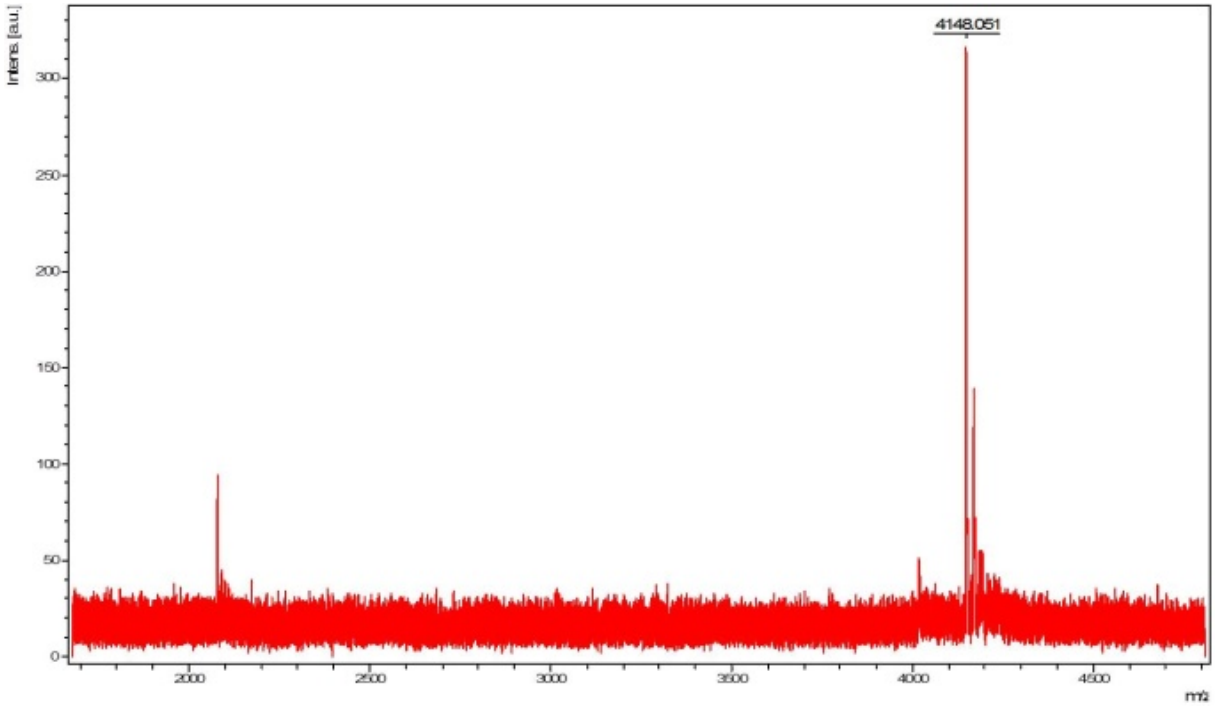

Figure S15. MALDI-ToF spectra of ODN3 (calcd. for $[M+H]^+$: 4148 Da).

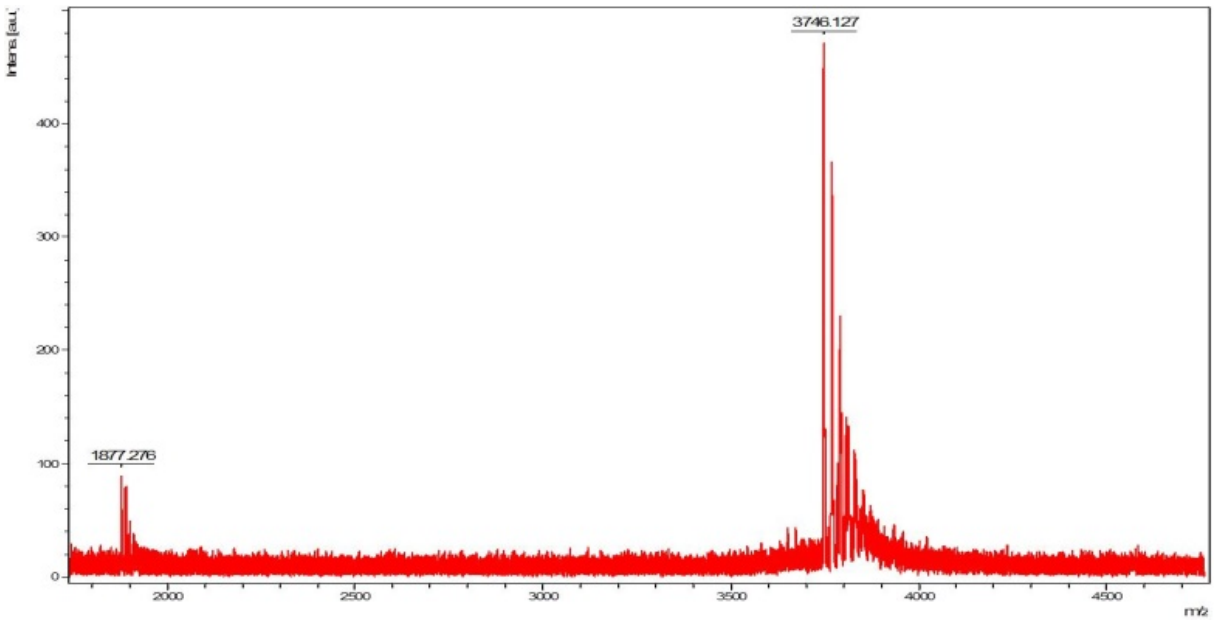

Figure S16. MALDI-ToF spectra of ODN4 (calcd. for $[M+H]^+$: 3744 Da).

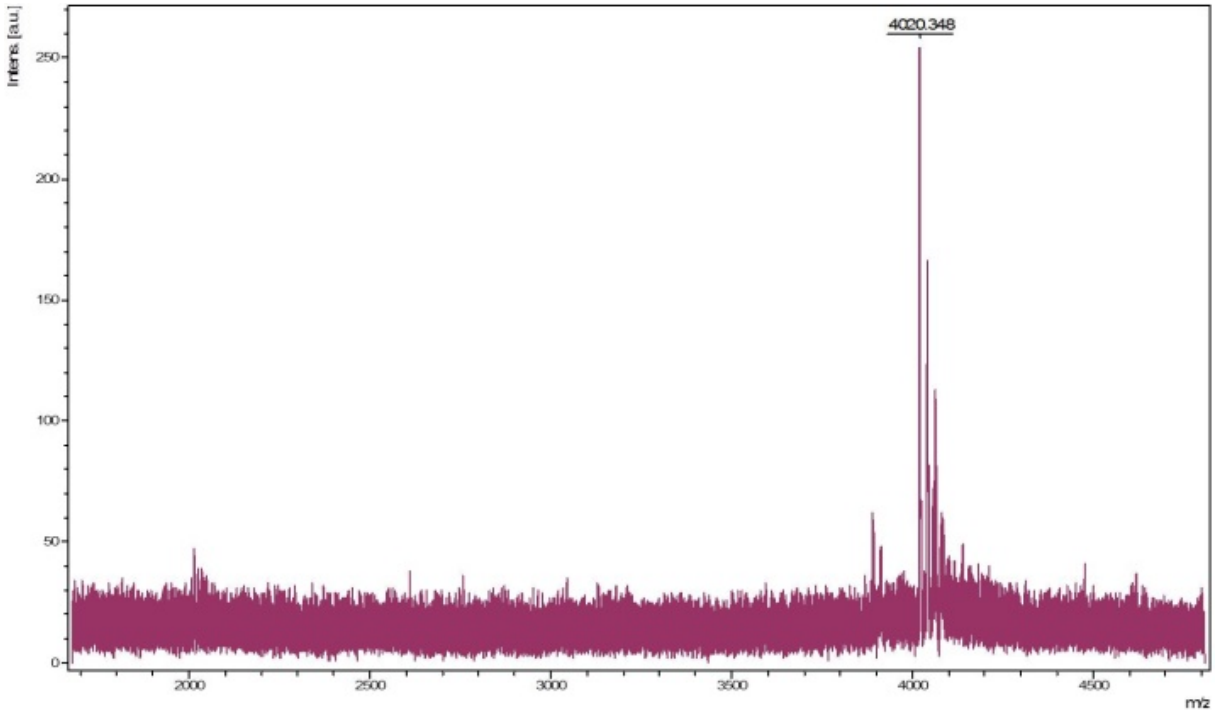

Figure S17. MALDI-ToF spectra of ODN5 (calcd. for $[M+H]^+$: 4020 Da).

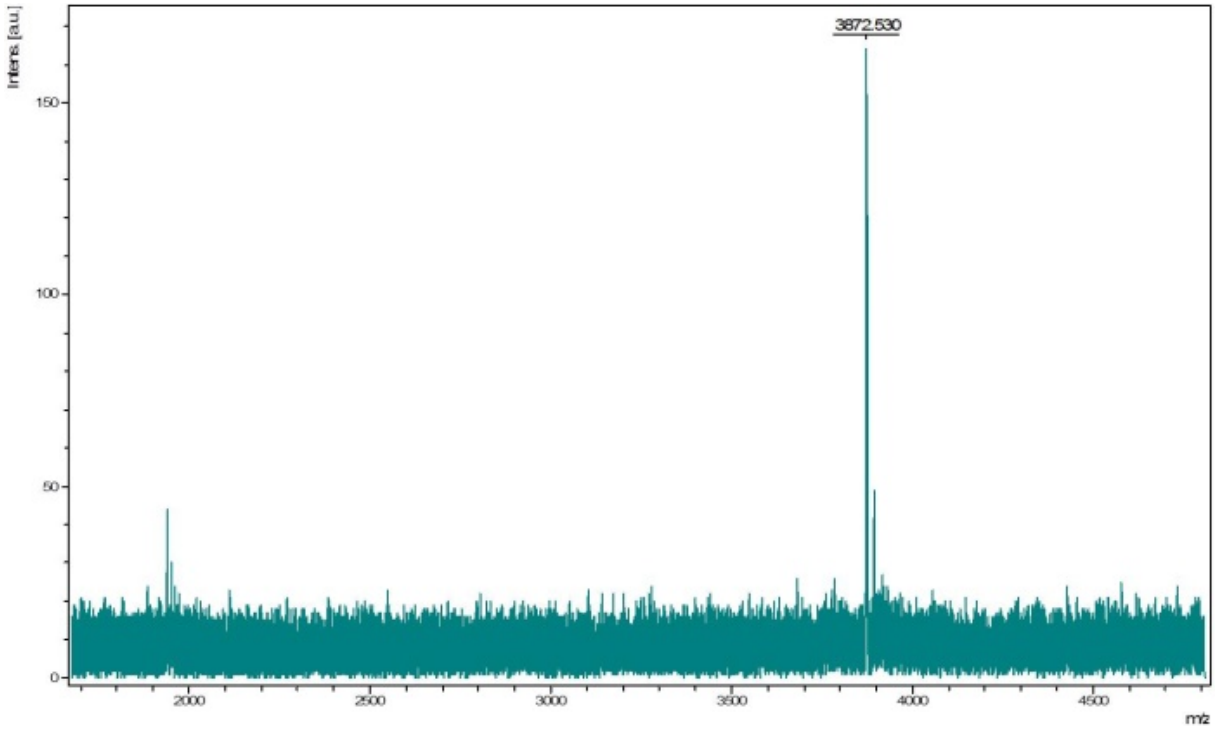

Figure S18. MALDI-ToF spectra of ODN6 (calcd. for $[M+H]^+$: 3872 Da).

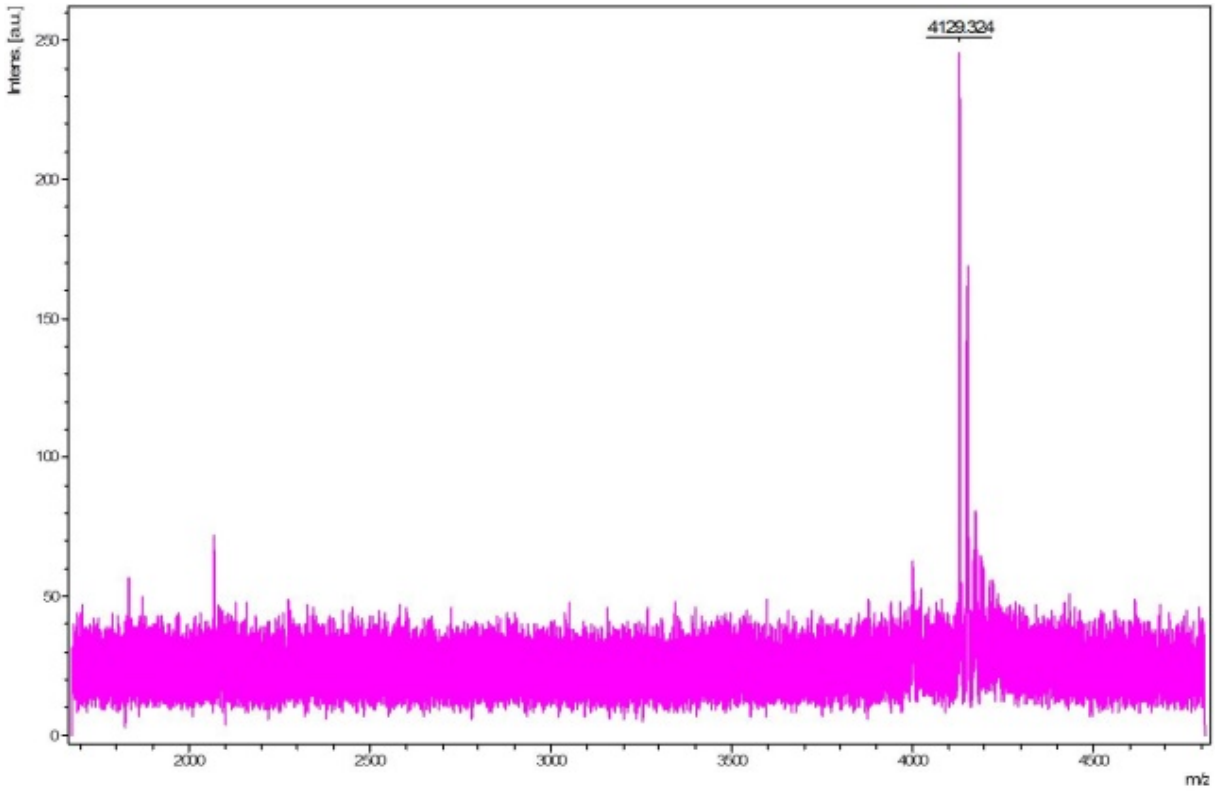

Figure S19. MALDI-ToF spectra of ODN7 (calcd. for $[M+H]^+$: 4129 Da).

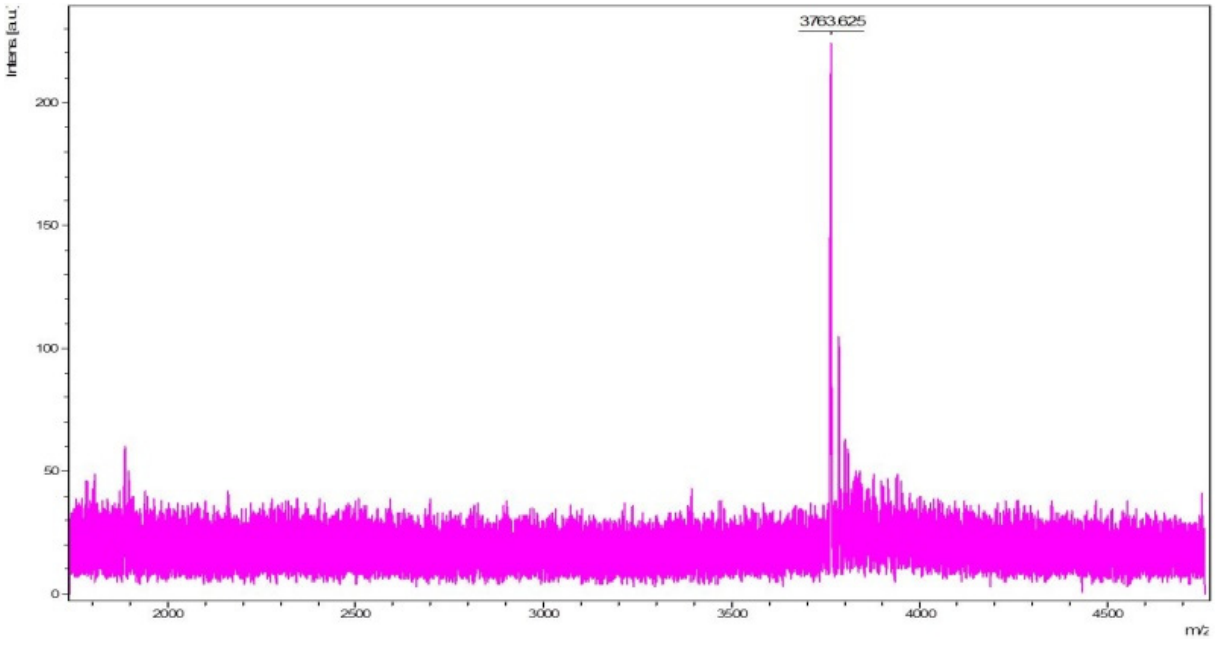

Figure S20. MALDI-ToF spectra of ODN8 (calcd. for $[M+H]^+$: 3762 Da).

References

[1] IUPAC-IUB Joint Commission on Biochemical Nomenclature, *Eur. J. Biochem.* **1983**, *131*, 9–15.